

Whole crustal response to late Tertiary extension near Prince Rupert, British Columbia

Lincoln S. Hollister*

Department of Geosciences, Princeton University, Princeton, New Jersey 08544, USA

John Diebold

Lamont Doherty Earth Observatory, P.O. Box 1000, Route 9W, Palisades, New York 10964, USA

Triparna Das

Department of Geosciences, Princeton University, Princeton, New Jersey 08544, USA

ABSTRACT

Crust-penetrating multichannel seismic data imaged crustal features of late Tertiary extension in east Dixon Entrance, British Columbia. The data show grabens as much as 3 km deep, mid-crustal west-dipping reflecting packages interpreted as normal sense shear zones, middle to lower crustal subhorizontal reflecting horizons, a generally reflective Moho, and arches of the Moho with relief of as much as 3 km (Moho depths 24.8–27.5 km). Based on dated extension-related features reported for the region, east-west extension occurred between 40 and 20 Ma and may have been concentrated between 25 and 20 Ma. If the pre-late Tertiary crustal thickness of east Dixon Entrance was the same as that of the mainland to the east (34 km), the minimum amount of crustal thinning in the study area was 30%.

Thinning of the whole crust above a stronger mantle lithosphere is implied by the extension-related features that we describe from the brittle upper crust down through the ductile lower crust to the Moho. Our data confirm and extend the interpretation of crustal extension by Lowe and Dehler and Dehler et al. for Hecate Strait and Queen Charlotte Sound. Integration of our results with the geologic history across the study area leads to a conclusion that preexisting zones of weakness may have controlled the pattern of crustal thinning during the extension.

Keywords: crustal extension, seismic reflectivity, Moho, British Columbia, tectonic reactivation.

INTRODUCTION

The 1994 ACCRETE offshore-onshore wide-angle reflection and refraction seismic experiment (<http://geoweb.princeton.edu/research/ACCRETE/accrete.html>) imaged features related to the accretion of terranes in western Canada (Morozov et al., 1998, 2001, 2003; Hammer et al., 2000; Hammer and Clowes, 2004; Rohr et al., 2000; Andronicos et al., 2003; Hollister and Andronicos, 2006). Included in the ACCRETE study was the collection of 1700 km of marine multichannel seismic (MCS) reflection data in the inland waterways of northern British Columbia and southeast Alaska (Rohr et al., 2000; Das, 1997; Figs. 1 and 2).

Previous geological and geophysical studies concluded that Miocene extension resulted in the opening of Hecate Strait and Queen Charlotte Sound (Fig. 2). Rohr and Dietrich (1992) used MCS reflection data to image extensional grabens in this region (Fig. 2). Dehler et al. (1997) integrated those seismic reflection data with seismic refraction, geologic, gravity, and heat-flow data (Hyndman and Hamilton, 1993; Lowe and Dehler, 1995; Spence and Asudeh, 1993; Spence and Long, 1995; Hickson, 1991; Woodsworth, 1991) to describe this extension.

Intersecting ACCRETE MCS reflection lines in east Dixon Entrance (Fig. 3) provide a crude three-dimensional image of 6000 km² of the crust. These profiles are described and interpreted in this paper. We tie our MCS results to the onshore-offshore wide-angle reflection and refraction results of Morozov et al. (1998, 2001, 2003) and describe the response of the whole crust of east Dixon Entrance to late Tertiary extension. Our results confirm and extend the evidence for Neogene extensional tectonics in

Queen Charlotte Sound and Hecate Strait; we describe the effects of the extension on the whole crust, and we infer that the pattern of response of the crust to extension may have been controlled by anisotropy in the crust formed during terrane accretion during the Mesozoic.

GEOLOGICAL AND GEOPHYSICAL SETTING

Hollister and Andronicos (2006) used the results of ACCRETE and those of previous studies to compile a geologic cross section (Fig. 4) from the interior of British Columbia to the Pacific Ocean. Included in their interpretation of this section is the recognition of the profound effects of an early Tertiary high-temperature extension event in forming the crust east of the Coast shear zone. This extension occurred while the rocks east of the shear zone were partially molten, and we assume here that extension of crust when the lower part was partially melted would lead to a relatively flat Moho. The map pattern for the Coast Mountains batholith (Fig. 1) outlines the region where the early Tertiary high-temperature extension likely occurred.

The Insular superterrane, which is composed of the Alexander and Wrangellia terranes, is to the west of the Coast shear zone (Fig. 1). Queen Charlotte Sound, Hecate Strait, and Dixon Entrance are bordered by islands and headlands underlain mainly by the Insular superterrane. The inferred boundary between Wrangellia to the southwest and the Alexander terrane to the northeast projects across our study area (Wheeler and McFeely, 1991; Fig. 1). During the mid-Cretaceous, units of the Insular superterrane within the study area

*Corresponding author: linc@princeton.edu

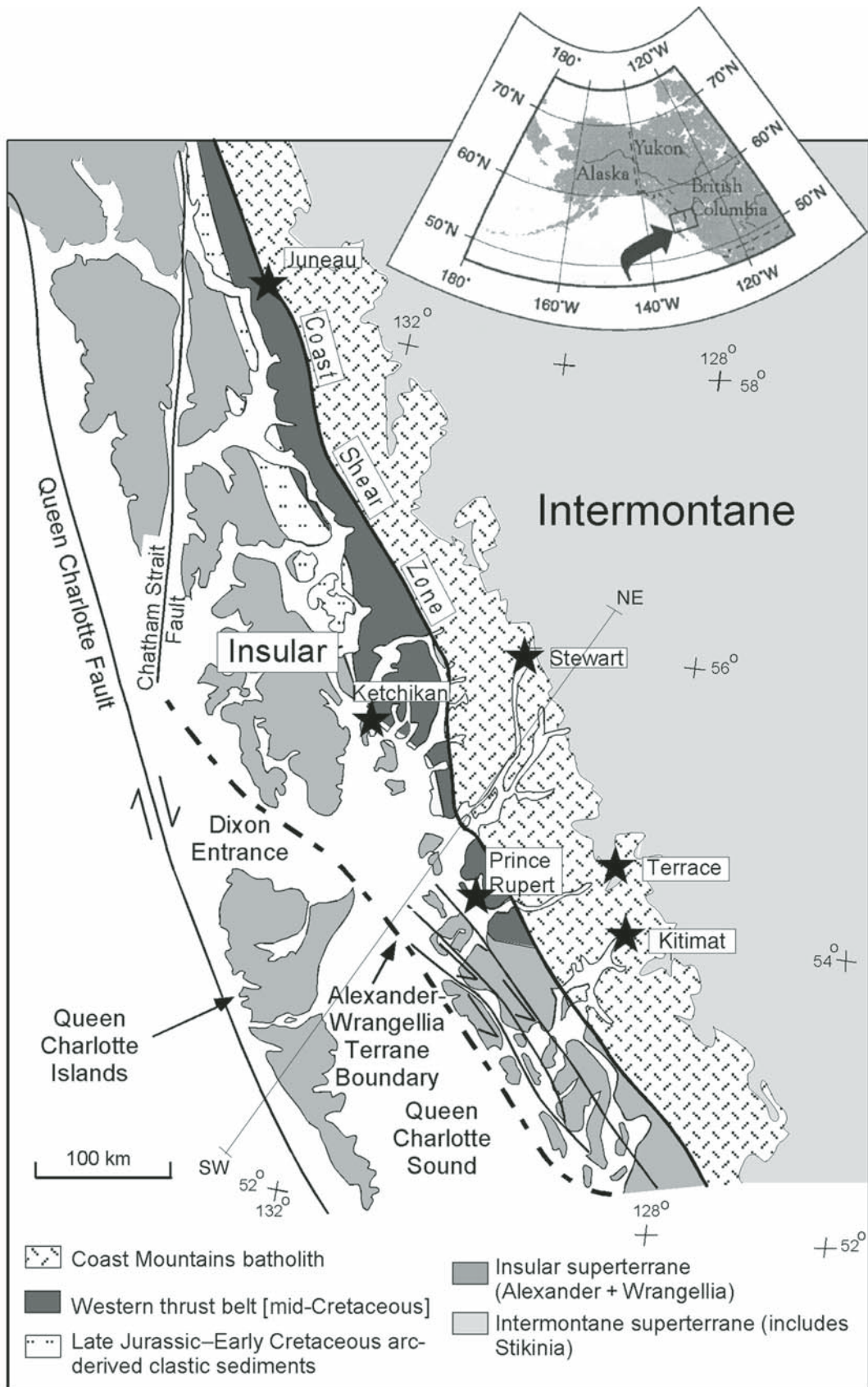


Figure 1. Regional map showing distribution of major geologic features of southeast Alaska and the north coast of British Columbia, and the location of the boundary between Wrangellia (southwest side) and the Alexander terrane (northeast side), after Wheeler and McFeeley (1991). Also shown south of Prince Rupert are three Mesozoic sinistral shear zones (Chardon et al., 1999) that project into the study area of east Dixon Entrance (see Fig. 3). SW-NE—line of the geologic cross section shown in Figure 4.

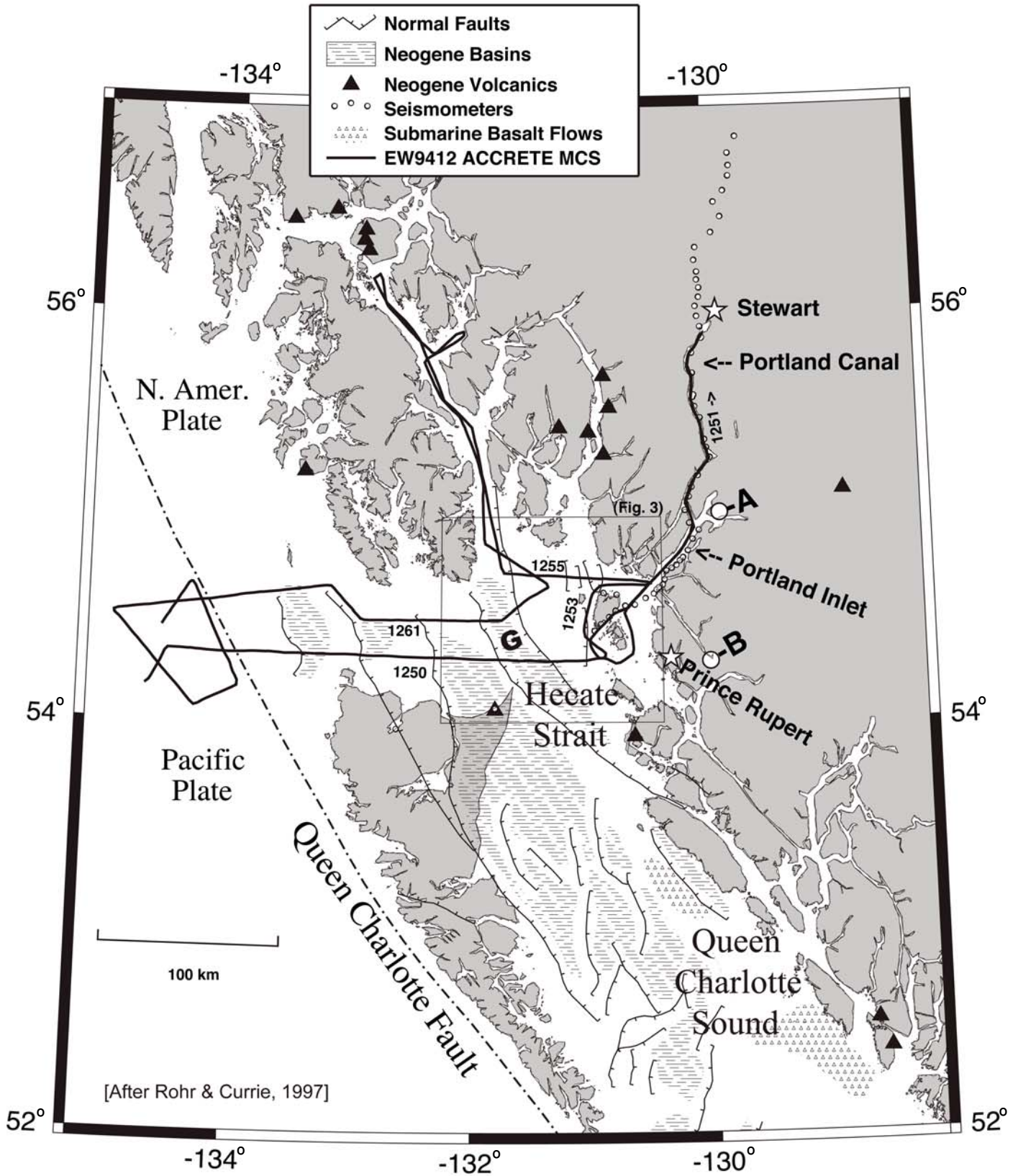


Figure 2. ACCRETE ship tracks (solid lines) and on-shore portable seismometer locations (small open circles). Numbers on ship tracks identify multichannel seismic (MCS) profiles. Shows area of Figure 3, the study area, grabens related to late Tertiary crustal extension (after Rohr and Currie, 1997), including those identified in this study, and late Tertiary sediment basins and extrusive volcanic rocks. Localities A and B are discussed in text. G labels a large graben described in text.

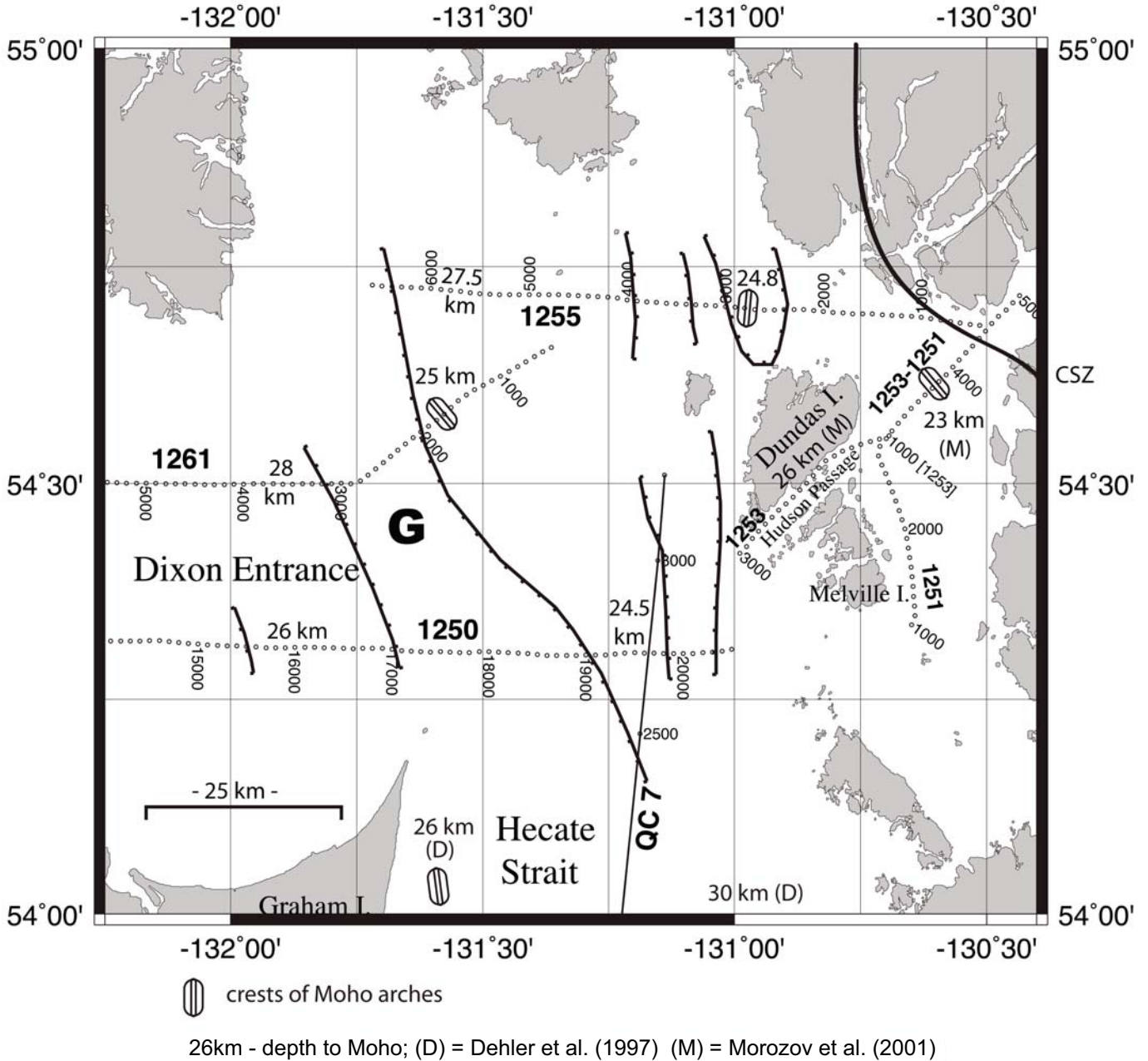


Figure 3. Common depth point (CDP) navigation of R/V *Maurice Ewing* profiles in east Dixon Entrance. Open circles indicate every 100th CDP. Line 1251 begins southeast of Melville Island and proceeds northward, and then turns northeast into Portland Inlet. Line 1253 begins along the same track (CDP 1000 of line 1253), and continues the profile of line 1251 southwestward through Hudson Passage. A segment of multichannel seismic (MCS) line QC7, from Rohr and Dietrich (1992), is shown as a solid line. Lines with bars show sides of grabens, barb on down-dropped side. Graben labeled G is described in text. Crests of Moho are indicated by symbol. Depth to Moho is indicated in kilometers; CSZ is Coast shear zone.

(Fig. 3) were imbricated in a ductile, thick-skinned, west-verging thrust package (Crawford et al., 1987; Rubin and Saleeby, 1992; Klepeis et al., 1998). South of the study area, the Insular superterrane is cut by major Mesozoic sinistral transpressive shear zones (Fig. 1;

Chardon et al., 1999) that strike into the waterways of the study area.

Although the rocks at the surface that are exposed on the islands and headlands of the study area (Fig. 3) belong to the Alexander terrane (with the exception of Graham Island

and the Coast Mountains batholith northeast of the Coast shear zone), the lower crust, below ~17 km, is likely Wrangellia (Morozov et al., 2001, 2003). Morozov et al. (2003) showed that the seismic P-wave velocity (6.9 km/s) and the ratio of P-wave to S-wave velocities (1.85) of

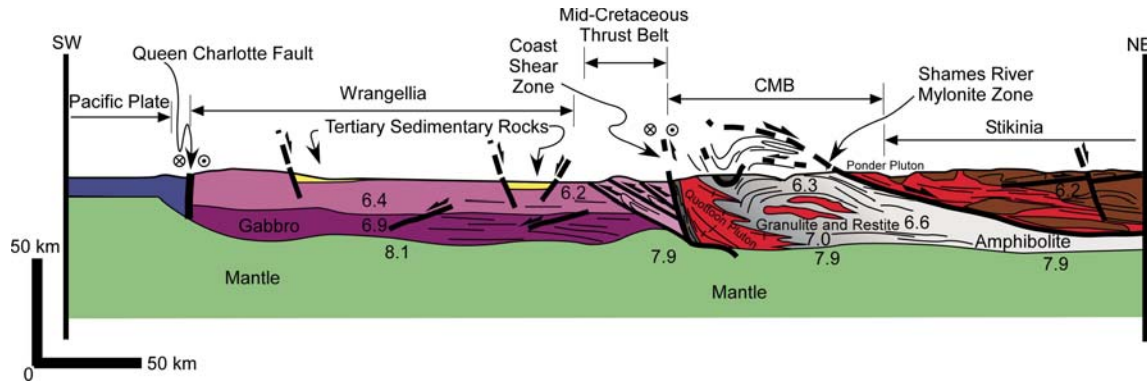


Figure 4. Generalized and simplified southwest-northeast cross section from the Pacific plate to the interior of British Columbia from Hollister and Andronicos (2006); the location of cross section is shown in Figure 1. Present-day lithologies, location of Moho, compressional wave velocities (V_p , km/s), major geologic features, and displacement directions across major shear and fault zones are shown. Note three arches of the Moho between the Queen Charlotte fault and the Coast shear zone (CSZ). The western arch was defined by gravity and wide-angle seismic reflection (Dehler et al., 1997); the central arch is based on that of line 1255 (Fig. 6); the arch west of the CSZ was defined by wide-angle reflection (Morozov et al., 2001). The portion of section labeled Wrangellia may include the Alexander terrane toward its northeastern limit. CMB—Coast Mountains batholith.

the lower crust between common depth points (CDPs) 19,000 and 20,000 on line 1250 (Fig. 3) correspond to gabbro. According to Lassiter et al. (1995), Wrangellia, which underlies most of the Queen Charlotte Islands, is a flood basalt province composed of basalt from a plume source that intruded into and through an island arc. The physical properties of the lower crust in the study area are thus consistent with intrusions associated with oceanic flood basalt and/or the middle crust of an island arc (Shillington et al., 2004). However, the seismic velocities of the upper crust of the study area are consistent with the felsic crust of the Alexander terrane (Morozov et al., 2001, 2003). This felsic portion of the crust thickens toward the east and reaches the Moho at the Coast shear zone (Fig. 4).

Dehler et al. (1997) described extension in Hecate Strait and Queen Charlotte Sound. They inferred that the extension occurred between 43 and 20 Ma based on the age range of late Tertiary basalts, which they attributed to decompression melting in the mantle due to unloading during the extension. These basalts are common in Queen Charlotte Sound and along its shores (Fig. 2; Hickson, 1991; Woodsworth, 1991; Hyndman and Hamilton, 1993; Rohr and Currie, 1997). The majority of these extension-related basalts extruded between 25 and 20 Ma, which led Dehler et al. (1997) to suggest that the extension may have been focused in this time interval.

Stock and Molnar (1988) and Rohr and Dietrich (1992) concluded that the area inboard of the Queen Charlotte fault underwent a period of transtension during the late Tertiary. Rohr and Dietrich (1992) argued that extension in Queen

Charlotte Sound and Hecate Strait was linked to transform motion along the Queen Charlotte fault, whereby the shear stresses along the fault were distributed across the continental margin as east-west extension and north-northwest dextral strike slip parallel to the Queen Charlotte fault.

The orientations, kinematics, and ages of brittle faults on land, to the east of east Dixon Entrance, help constrain the stretching direction of the late Tertiary extension. According to Evenchick et al. (1999) and van der Heyden et al. (2000), an extensional structure parallels and includes the north-south trend of Portland Canal (Fig. 2), which probably formed by glacial erosion along a brittle fault system (Evenchick et al., 1999) associated with this structure. This faulting must have occurred after the rocks of the Coast Mountains batholith, now exposed at the surface, had cooled through the brittle-ductile transition, which took place ca. 48 Ma, according to Hollister (1982) and Andronicos et al. (2003).

At locality A (Fig. 2), north-south-trending nearly vertical faults are on strike with the north-south trend of Portland Canal, and they cut the ductile fabric of the gneiss of the Coast Mountains batholith. These faults have slickensided surfaces and striations indicating east side down displacement and east-west extension. The faults are cut by vertical, northeast-trending basalt dikes that have been assigned ages from 45 to 20 Ma (Gareau et al., 1997; van der Heyden et al., 2000; Evenchick et al., 1999). At locality B (Fig. 2), psuedotachylites, which form during rock displacement that is rapid enough to cause local melting, occur in a dextral strike-slip fault zone within the Coast shear zone, which strikes

parallel to its north-northwest trend; Davidson et al. (2003) dated them as 29.8 Ma, using the Ar/Ar method. The age, orientation, and displacement direction of the faults at localities A and B provide a complimentary data set to the proposed regional late Tertiary extension described and discussed in this paper.

DATA ACQUISITION AND PROCESSING

The ACCRETE EW9412 seismic profiles together compose a transect from the Pacific plate, across the Queen Charlotte fault zone (Rohr et al., 2000), the Wrangellia and Alexander terranes, the Coast shear zone, and north-eastward up Portland Inlet and Portland Canal to Stewart, British Columbia (Fig. 2). The interpretations in this paper are based on the loose grid of MCS profiles shot in relatively shallow water of east Dixon Entrance (Fig. 3). The air-gun pulses were also recorded by an onshore seismograph array deployed from Dundas Island to Stewart and in line with Portland Canal north of Stewart (Fig. 2) (Morozov et al., 1998, 2001, 2003; Hammer et al., 2000; Hammer and Clowes, 2004).

The seismic source was an 8500 in³ 20 airgun array, which was towed by R/V *Maurice Ewing*, as was a 240 channel, 3000 m digital hydrophone streamer. This equipment was deployed in the deep water west of the Queen Charlotte fault zone (Fig. 2), and profiling proceeded eastward. Because of the need to tow and maneuver the hydrophone array all the way into the freshwater at the head of Portland Canal, the array was shortened from its usual 4000 m to 3000, and it

was rebalanced, to match the lower density of freshwater. From the Queen Charlotte fault zone to Melville Island (line 1250, Figs. 2 and 3), it was difficult to control the depth of the hydrophone array, and it tended to tow close to or at the sea surface, resulting in noisy and weak data quality. The array performed as desired within Portland Canal (line 1251). Upon reentering Dixon Entrance, the array was rebalanced again, to a density more suitable for seawater. As a result, the reflection lines 1253, 1255, and 1261, collected subsequent to line 1251, are of higher quality than line 1250.

The difficulties of acquiring reflection seismic data in fjords and fjord-like environments are well known (cf. Hurich, 1996; Hurich and Roberts, 1997; Brady et al., 2000). Echoes from the rocky walls of these channels are nearly impossible to discriminate from the desired vertically traveling arrivals, and reverberations from hard bottoms in a shallow water column are common. Virtually all of our recorded data were dominated by waterborne diffracted energy. Similar effects were also described by Hurich (1991). Data processing began, therefore, with the elimination of noisy traces and two-dimensional (F-K) velocity filtering of shot gathers, which eliminated much of the waterborne energy arising from diffractions from the bottom and sides of the various waterways. This filtering, however, is ineffective at small source-receiver offsets, where the primary reflections and the water-column multiples are indistinguishable, and in the upper section, where data with larger source-receiver offsets cannot be included in the stacks. The shot gathers were then sorted into CDP gathers spaced 12.5 m apart. Poststack processing included a further velocity filtering pass and deconvolution. Coherence was enhanced by dip-adaptive trace mixing, as well as the usual enhancements afforded by bandpass filtering and trace gain adjustments. The result of this processing was that the effects of waterborne diffractions were confined to the upper 1–2 s of the profiles in most cases, revealing mid-crustal reflectors in many locations. Reflection Moho can also be tracked in most of the profiles.

Self-consistent prestack static corrections were applied before CDP gathering, and these tended to increase the coherence of crustal reflections at the expense of the reverberation noise. These were based on a model of the seafloor and of the crystalline basement-sediment interface that was derived from preliminary brute stacks of the data (Das, 1997). Although routinely done in onshore reflection processing, this was an unusual step for processing marine reflection data.

The uppermost sedimentary sections are well imaged in simple, non-static-corrected

stacks (e.g., Fig. 5), whereas the uppermost crustal structures are poorly resolved, due to reverberations and the scattering effects of the rough sediment-basement interface. When the scattering effects are ameliorated by prestack static corrections, the sedimentary sections are distorted, because the traces were shifted by the computed statics time corrections prior to stacking. This procedure improved the coherence of the reflectors at depth (e.g., Fig. 6) at the cost of the loss of the continuity of the seafloor reflections and the reflections within the top few hundred milliseconds of the surface.

Poststack time migration was carried out on most of the stacked sections, but this process tended to smear seismic noise arising from the various sources described above, making the images more difficult to interpret. Accordingly, we used the technique known as line migration. We digitized the profile interpretations on the prestack static corrected sections, using the stacking velocity functions, and migrated the digitized reflectors (e.g., Fig. 7) to move them into their original physical positions. This process assumes that all of the reflections come from within the plane of the seismic profile. None of the digitized reflectors was moved far enough by this process to affect our interpretations. In order to estimate depth of the digitized horizons, the velocity function determined by Morozov et al. (1998, 2001) was used in a similar procedure. The easternmost velocity function presented by Morozov et al. (2001, their Fig. 6) was specified for the zone between 20 km and 40 km east-southeast from the southeastern tip of Dundas Island. This corresponds roughly to CDPs 19,200–20,000 of line 1250 (Figs. 3 and 5). Since this is the only place that the Morozov et al. (2001) model overlaps with the area studied in the current paper, it was applied, after combination with the water and sediment column models determined from the MCS data. In this way, the distorting effects of variations in the upper section (such as grabens) were minimized.

SEISMIC REFLECTION OBSERVATIONS

In the sections below, we refer to the profiles that best illustrate the features discussed.

Reflection Moho

In line 1255 (Fig. 6), the Moho reflection is prominent at 8–9 s two-way traveltime (TWTT) and is in the shape of an arch with ~1 s amplitude; the apex of the arch is at approximately CDP 2800. The Moho reflection is also promi-

nent along line 1253 (Fig. 8). Morozov et al. (2001) reported a depth to the Moho of 26 km at about CDP 2600, where the MCS image of the Moho is at 8.5 s TWTT. Given that the lower crust of the Insular superterrane has a velocity of 6.8 km/s (Morozov et al., 2001), the arch of line 1255 (Fig. 6) has an amplitude of ~3 km, from 24.8 to 27.5 km. Although the character of Moho reflections is variable, the position and shape of the Moho are clear.

There are several intervals of laterally continuous, high-amplitude reflectivity that define the Moho, and one interval of especially high amplitude reflectivity around CDP 5000 (unmigrated). This interval is highly reverberant, suggesting the presence of layering with high-velocity contrasts. The fact that similar reverberation is not apparent in the overlying crustal, seafloor, or sediment reflections indicates that its origin is local to the reflection Moho. Besides the interval of relatively high reflectivity on Moho of line 1255, there are also intervals of relatively high amplitude reflectivity on line 1261 at CDP 1600 (Fig. 7) and on line 1250 at CDP 19,000 (Fig. 5).

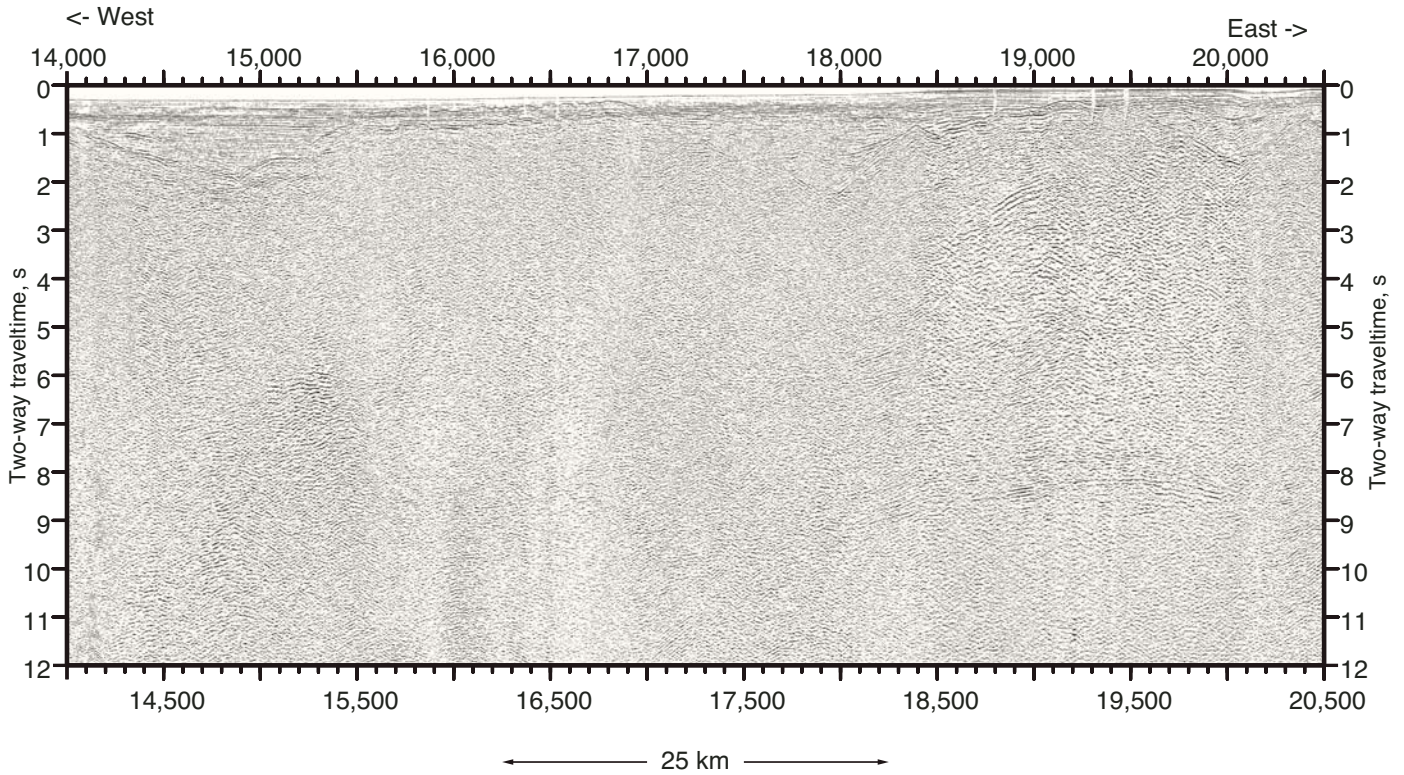
Moho on line 1261 (Fig. 7) appears also to have an arch; its apex is at CDP 1700, at a depth of 25 km. Moho deepens to the west from this arch to a keel at a depth of 28 km at CDP 3500.

Middle to Lower Crustal Reflectivity

Mid to lower crustal discontinuous, subhorizontal (in line of section) reflectors (> 5 s TWTT, or ~15 km) are prominent in the profiles shown in Figures 8 and 9. Apparent west-dipping packages of reflectivity are present in Figures 5, 6, and 8. On the profile of line 1255 (Fig. 6), one prominent group of reflectors (CDPs 3600–5400) has apparent dips to the west in the line of section. A second, less prominent, west-dipping group is between CDPs 1000 and 2000. These west-dipping reflecting packages extend from ~3 s TWTT (~9 km in depth) to almost 6 s TWTT (~18 km in depth). Based on the velocity model of Morozov et al. (2001) the maximum apparent dip of these reflectors is ~15°.

Because of the crude three-dimensional coverage in the study area, we can constrain the three-dimensional orientation of some of the reflecting horizons. Portions of lines 1251 and 1253 (Figs. 1 and 3) are merged into one continuous line (Fig. 8) from the Coast shear zone through Hudson Passage, in line with Portland Inlet (Fig. 2). In Figure 8, CDPs are shown for line 1251 from 5000 to 3000 (northeast half of figure) and for line 1253 from 1000 to 3000 (southwest half of figure). The portion of the seismic section through Hudson Passage (Fig. 3) shows a southwest-dipping (in line

EW9412 Line 1250



EW9412 Line 1250

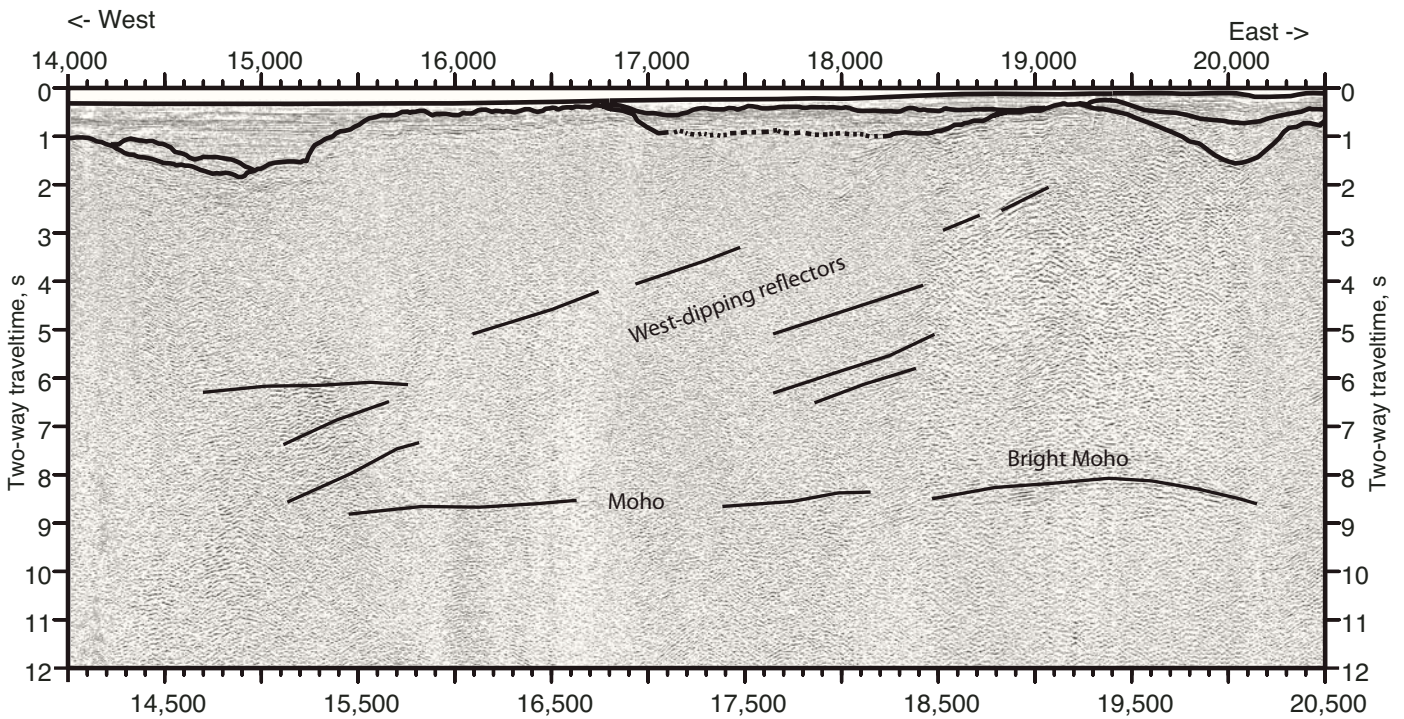
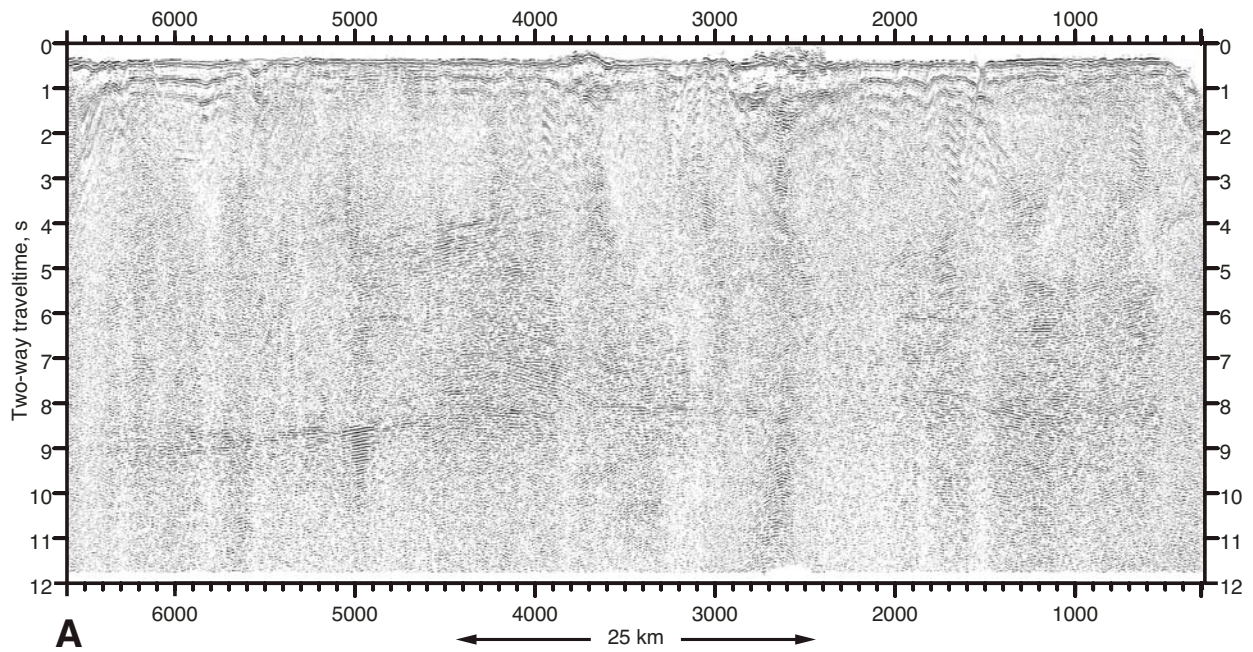


Figure 5. Common depth point (CDP) stack of line 1250, data (top) and interpretation (bottom). The graben between CDPs 17,000 and 19,000 is the southern continuation of one crossed by line 1261 (Figs. 2 and 7). A second graben is intersected between CDPs 14,000 and 15,500, and a third between 19,500 and 20,500. A package of mid-crustal west-dipping (in plane of section) reflectors is visible between CDPs 17,500 and 19,000. The Moho has a bright reverberant interval around CDP 19,000. The apparent arch in the Moho between CDPs 18,500 and 20,000 is not present following migration.

EW9412 Line 1255 CDP#



East Dixon Entrance

EW9412 Line 1255 CDP

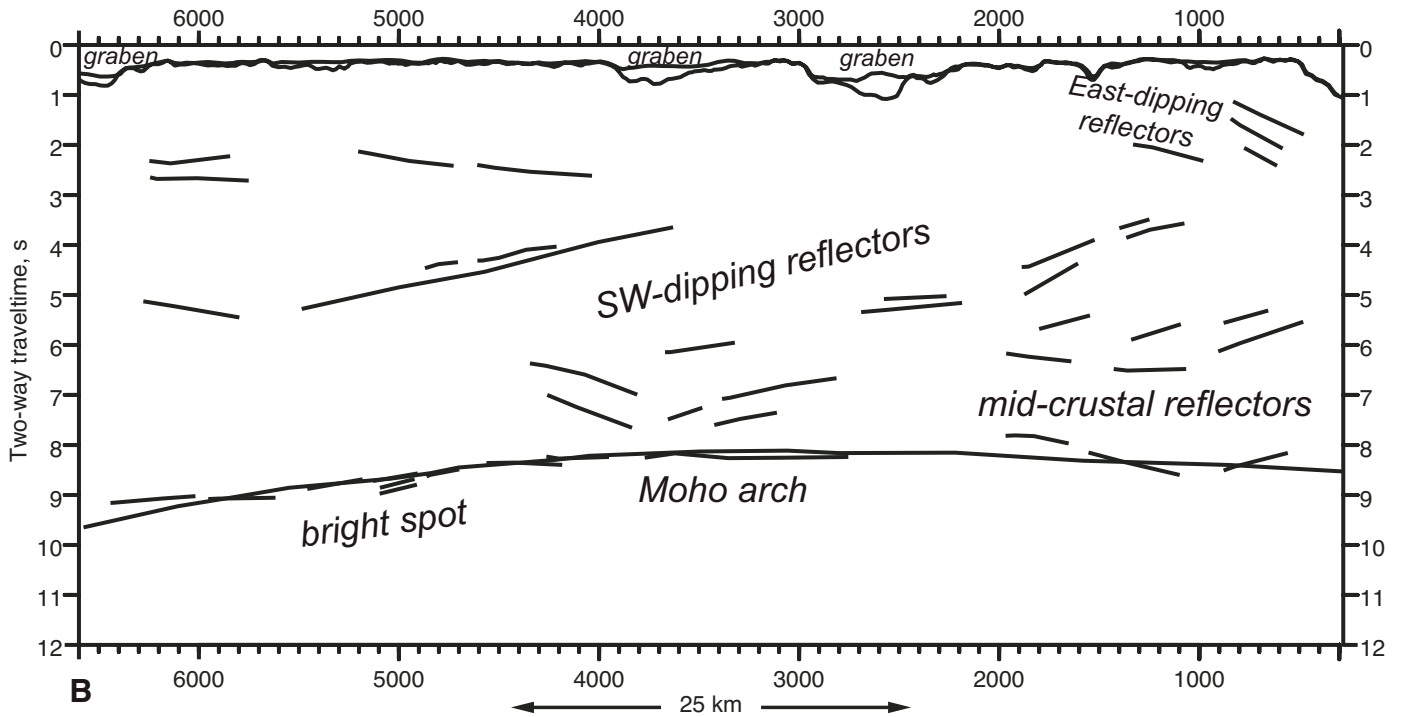
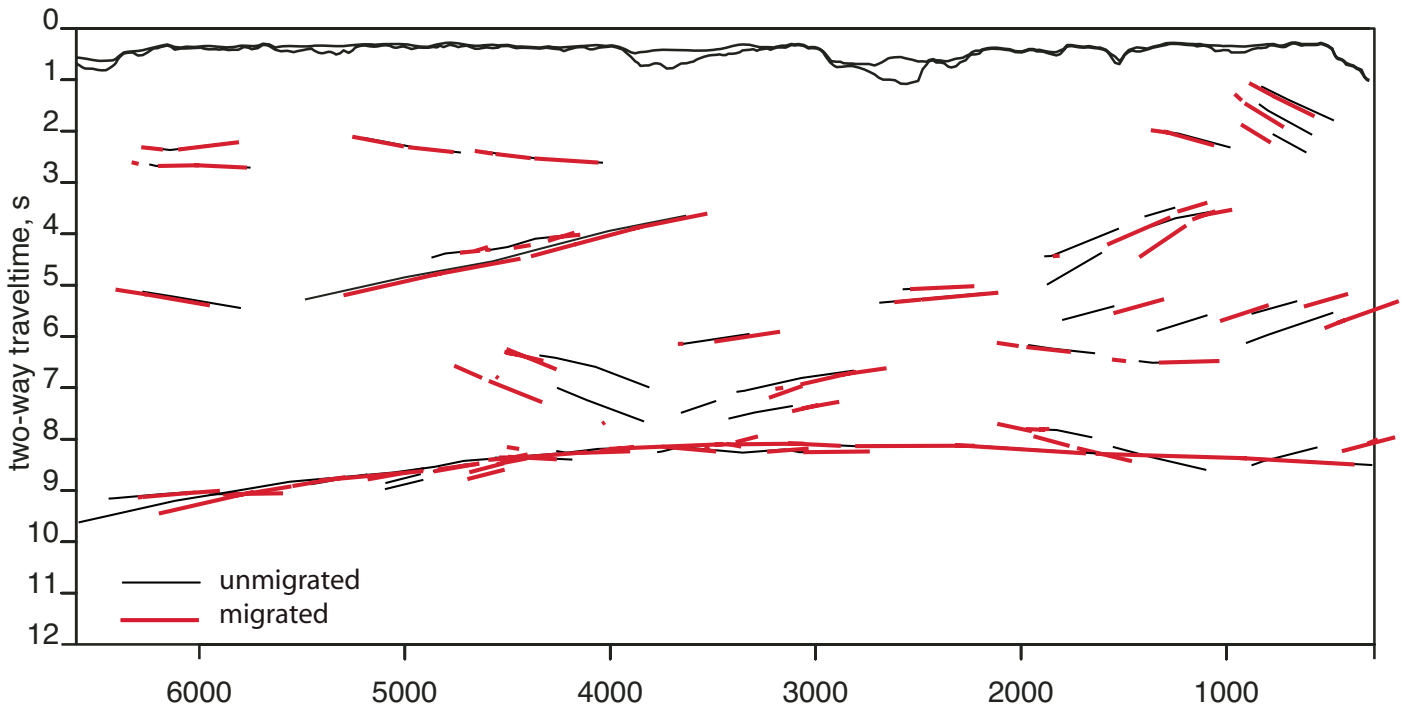


Figure 6. (A) Seismic profile for line 1255. Prestack statics corrections have been applied to enhance the coherence of crustal reflectors (Das, 1997). Those include strong, west-dipping mid-crustal reflection packages between common depth points (CDP) 3600 and 5400, and between CDPs 1000 and 2000. The strongest mid-crustal reflector, at ~4 s two-way traveltime (TWTT), between CDPs 3800 and 5400, dips westward at ~15°. East-dipping reflectors occur at 3–4 s TWTT between CDP 600–1200. The reflection Moho defines a smooth arch, with a very bright reverberant section around CDP 5000. Subhorizontal lower crustal reflectors are apparent below 5 s TWTT. The absence of reflecting packages, for example between CDPs 2000 and 2500, is likely due to interference from shallow structures (Peddy and Hobbes, 1987). (B) Line drawing interpretations of reflecting horizons of A. (Continued on following page.)

East Dixon Entrance



EW9412 Line 1255 CDP #

East Dixon Entrance

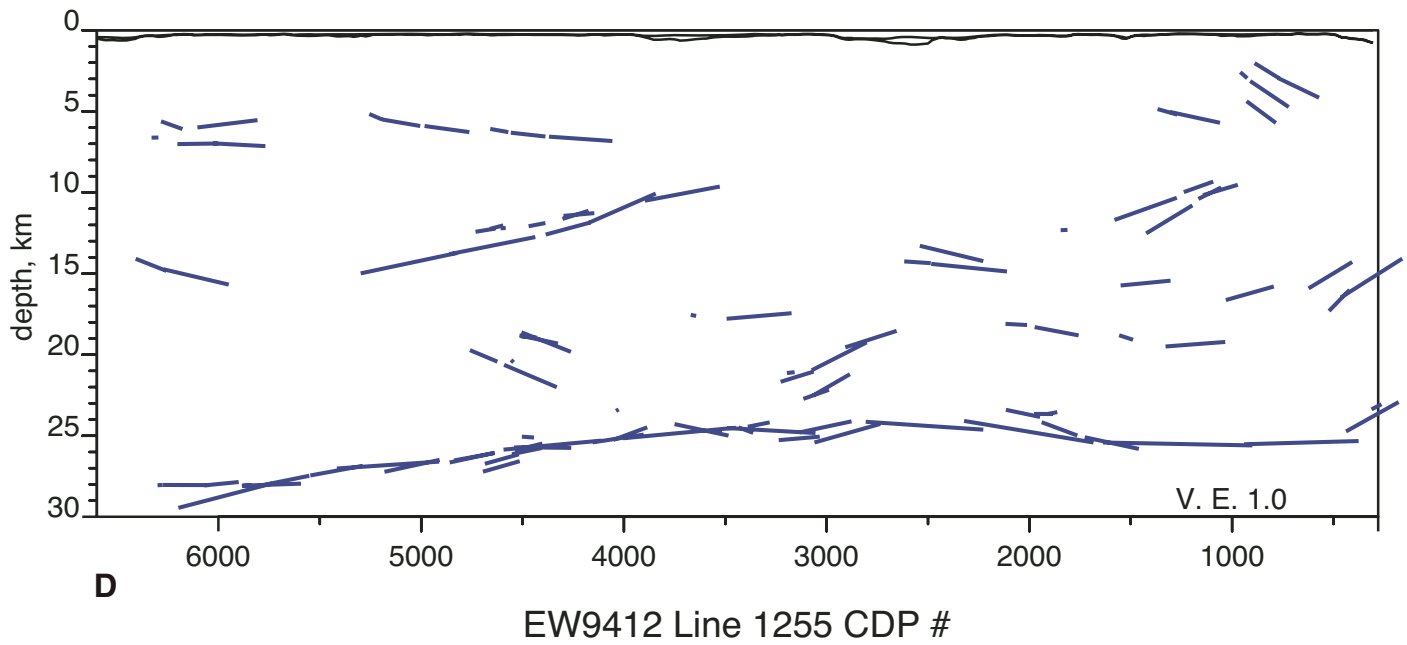


Figure 6 (continued). (C) Line drawings of the crustal arrivals in B (shown in black) have been migrated, using the velocity function of Morozov et al. (2001), and shown in red. Each individual line segment in the digitized horizons is migrated separately, and their positions may diverge, as dipping arrivals migrate updip in proportion to their observed dips. (D) The migrated line segments of C are converted to depth, again using the Morozov et al. (2001) velocity function. Despite the distorting effect of the two grabens labeled in B, the Moho arch is retained.

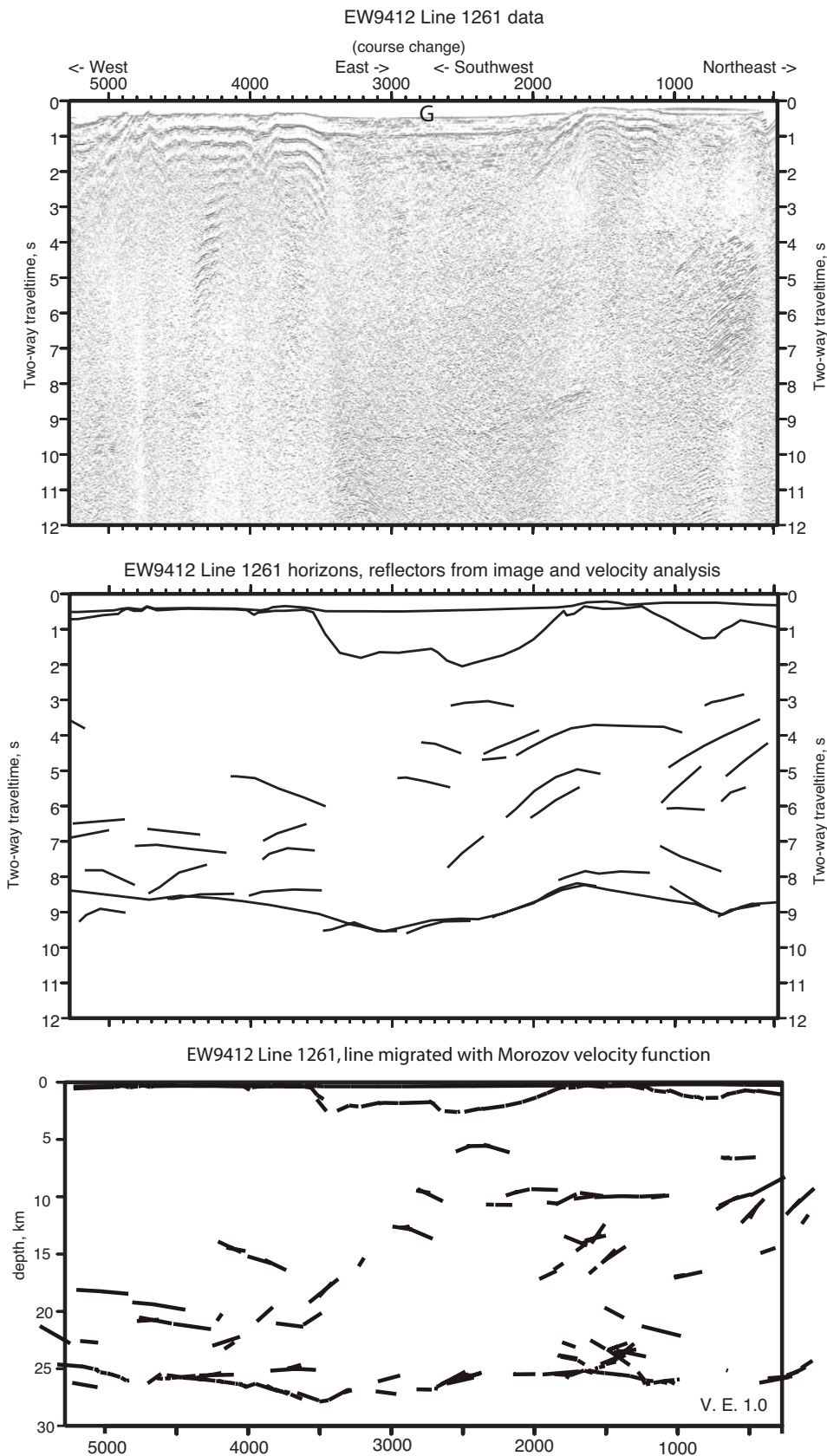


Figure 7. Line 1261. Top panel: processed data. As shown in Figure 3, this profile includes a course change as it passes over a sizeable graben (G), located between common depth points (CDPs) 1800 and 3500. Due to strong reverberations over thinly sedimented sections and weather-induced shallow towing of the hydrophone array, data quality is poor. Nonetheless, the Moho is detectable from place to place, particularly beneath the graben, where reverberations are minimized. Middle panel: line drawing interpretation of reflecting horizons of line 1261. Depth to the graben floor is constrained by analysis of refracted and wide-angle reflected arrivals in shot gathers. Lower panel: line segments of the horizons picked in middle panel have been migrated, using the velocity function of Morozov et al. (2001). In the lower panel, the migrated arrivals are plotted at the same horizontal scale as in the other panels, but the vertical scale is in kilometers, with no vertical exaggeration. The graben is thus determined to have a depth of 2.75 km, and the Moho depth varies from 25 to 28 km. This process was used to determine Moho depths for all the EW9412 profiles presented in this paper.

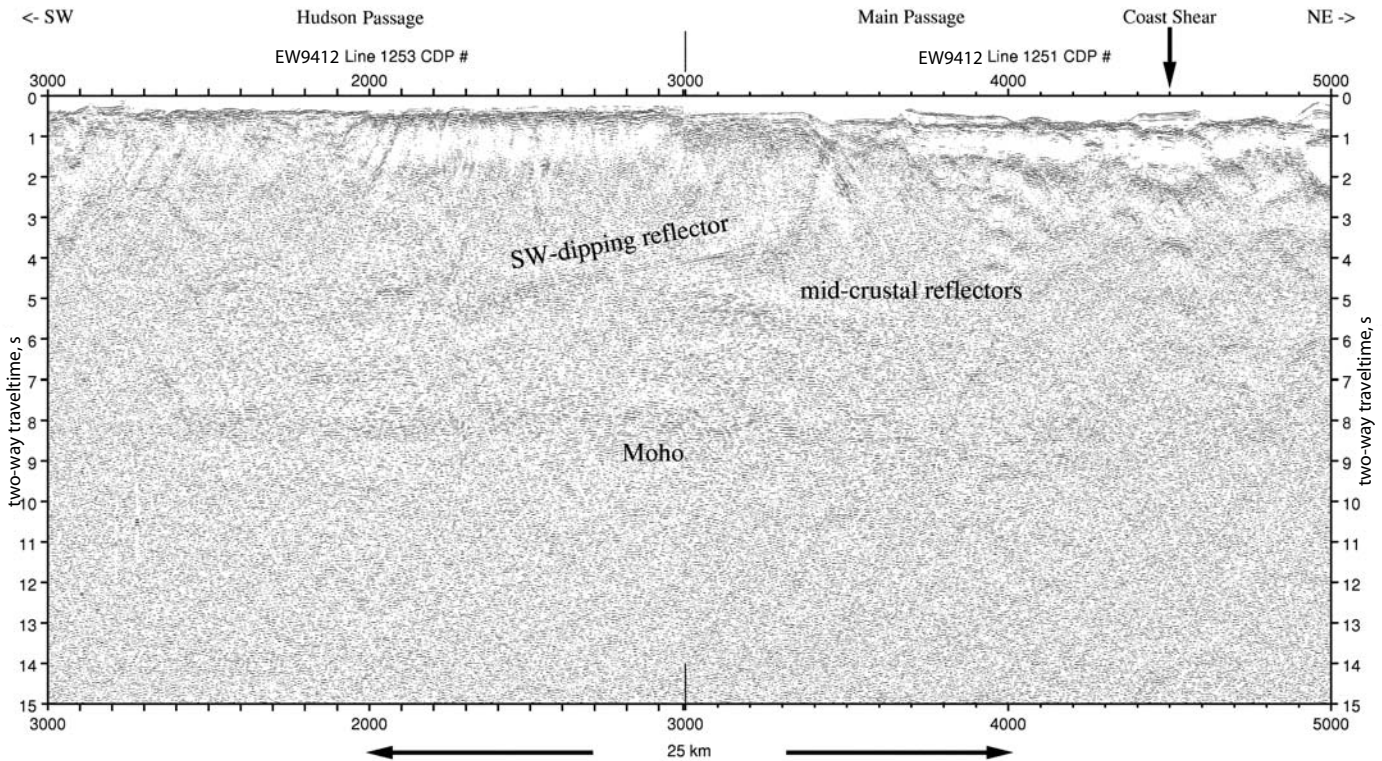


Figure 8. Common depth point (CDP) stack of line 1251–1253. Two line segments are juxtaposed, showing the continuity of the southwest-dipping (in line of section) mid-crustal reflector beneath Dundas and Melville Islands. Middle and lower crustal subhorizontal reflections are prominent at depths >5 s two-way traveltime (TWTT); the Moho is well imaged.

of section) reflector (Fig. 8) from a depth of 3 s TWTT down into a zone of horizontal (in line of section) mid-crustal reflectors at ~ 6 s TWTT (about CDP 2200 on line 1253). However, where line 1251 trends nearly north along the east side of Melville Island (south of CDP 3000; Fig. 9), there are no dipping reflectors; where the line turns to a northeast trend there is a southwest-dipping reflector. In Figure 8, this same reflector merges with the southwest-dipping reflector on line 1253. The portion of line 1253 (not shown) that trends north, along the west side of Dundas Island (Fig. 2), also has apparent subhorizontal lower crustal reflectivity, which is similar to that illustrated on the north-trending portion of the profile shown in Figure 9 (CDPs 1000–3000). Because the nearly north-south segments of lines 1253 and 1251 do not show dipping reflectors, and because the east-west lines (Figs. 5 and 6) and northeast-southwest lines (Fig. 8) do show dipping reflectors, the resolved dip of the reflectors is toward the west, with a strike line nearly north-south.

East-dipping reflecting horizons occur between 3 and 4 s TWTT at the eastern end of

line 1255 (Fig. 6), near CDP 600–1200. A fabric with this orientation was also imaged by the wide-angle seismic reflection experiment of Morozov et al. (2001).

Grabens

Grabens were clearly imaged in the standard CDP stacks of lines 1255 (Fig. 6), 1250 (Fig. 5) and 1261 (Fig. 7). Simple non static-corrected stacks enhance shallow sedimentary sections and this was done for profiles 1250 and 1261. Three grabens are shown in Figure 5. The graben on line 1261 (Fig. 7), between CDPs 1800 and 3400, has ~ 3 km of sediment fill based on its depth in TWTT of 2 s. For line 1250 (Fig. 5), the graben between CDPs 17,000 and 19,000 likely connects with the one imaged on line 1261 to the northwest and one imaged to the southeast on QC7 (CDPs 2400–2000; Rohr and Dietrich, 1992). These are connected in Figure 2 and labeled G. The eastern side of the same graben is imaged on line 1255 at CDP 6400, but this is not clear in Figure 6 because this profile was not processed to image shallow features.

DISCUSSION OF FEATURES ATTRIBUTED TO LATE TERTIARY EXTENSION

Figure 10 shows a compilation of our imaged features on an idealized east-west profile. The figure shows the arch in the Moho that is clearly imaged on line 1255. The Moho is reflective, and an interval below the Moho of high-amplitude reflectivity is also shown (bright spot). Packages of west-dipping reflectors occur in the middle crust, and the lower crust has reflectors subparallel to Moho, especially toward the eastern portion of the profile.

The relatively high reflectivity of the Moho may be due to shearing at the mantle-crust boundary during extension. In observations of other extended terranes, extension Moho typically appears as a narrow band of generally continuous reflections. Hammer and Clowes (1997), in reviewing occurrences of Moho reflections in the Canadian Lithoprobe transects, found that the strong, coherent Moho reflections appeared to be in zones where whole crustal deformation has been recognized, including crustal extension. Strain localized

East of Melville Island

EW9412 Line 1251

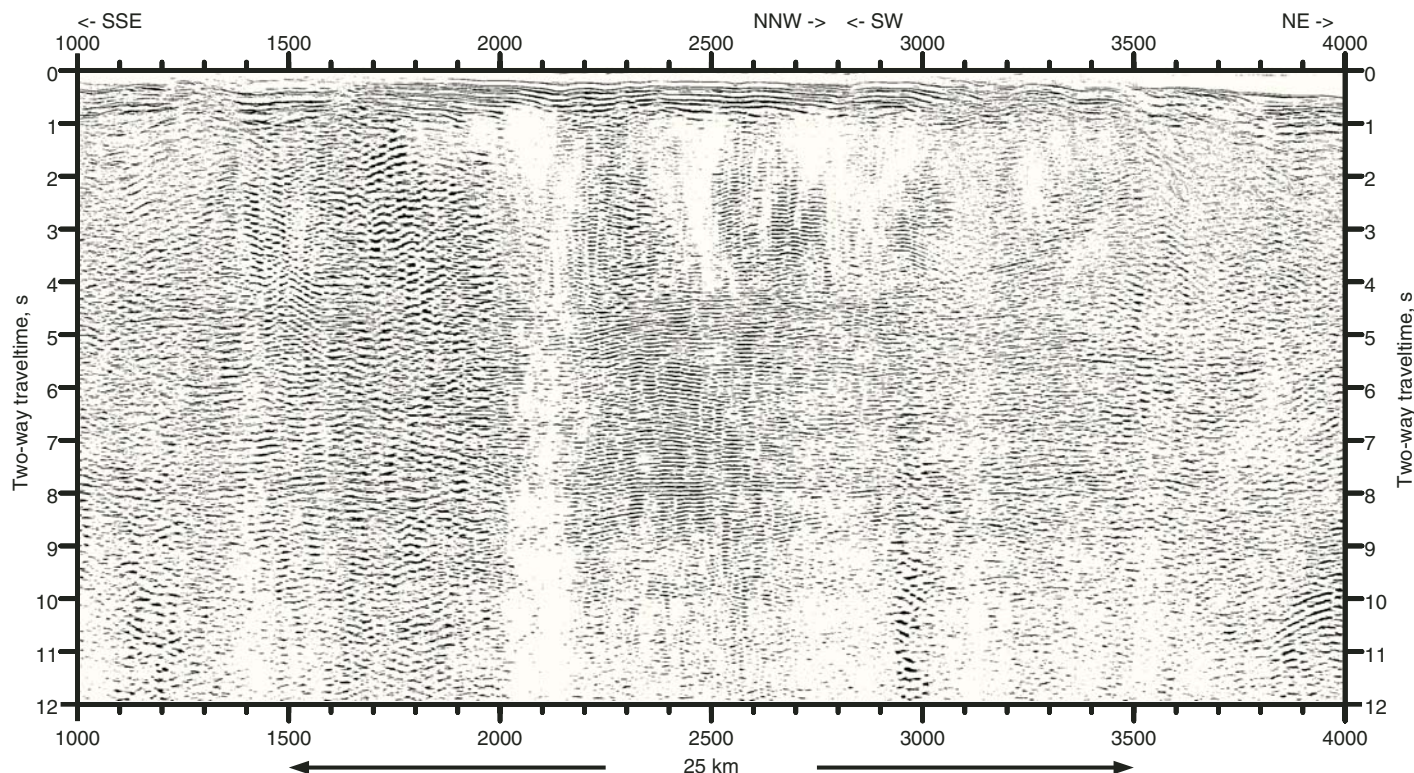


Figure 9. Portion of line 1251 extending parallel to eastern shore of Melville Island from common depth point (CDP) 1000–2900; at CDP 2900, the track turns northeast, beginning the southwest-northeast crossing of the Coast shear zone into Portland Inlet. Subhorizontal middle and lower crustal reflections are plentiful below 4.8 s two-way traveltime (TWTT). The mid-crustal southwest-dipping (in line of section) reflectors occur only between CDPs 2900 and 4000, where the line is northeast-southwest. The reflections are subhorizontal where the line trends north-south, between CDPs 1000 and 2900, showing that the true dip of the reflectors is to the west.

at the crust-Moho discontinuity could result in sharpening the velocity gradient, and shearing within the transitional zone would enhance reflective properties.

One interpretation of the high-amplitude reflective intervals on the Moho is that they could be due to where basalt accumulated below the crust-mantle interface after rising through the mantle lithosphere. The occurrences of late Tertiary volcanism (Fig. 2), which Rohr and Currie (1997) and Dehler et al. (1997) argued result from decompression melting during the late Tertiary extension of the region, support the inference that the high-amplitude reflective intervals could represent accumulations of solidified basalt within upper mantle peridotite.

We interpret the west-dipping reflecting horizons to be ductile normal sense shear zones produced during east-west extension. There are no west-dipping structures on the islands and headlands that surround and lie within the study area. In contrast, the prevailing dip of the

mid-Cretaceous rock fabric on shore is toward the northeast or east (Hutchison, 1982; Klepeis et al., 1998; Gehrels, 2001). If the west-dipping mid-crustal fabric (Fig. 10) is due to ductile shearing, the fact that it is not observed at the surface implies it is relatively young; i.e., there has not been enough exhumation to bring rocks to the surface that were below the brittle-ductile transition during the late Tertiary.

Dipping horizons that are oriented parallel to the extension direction were described by Peddy and Hobbes (1987) for offshore southwest Britain. These are in the same depth range as those we imaged. Lie and Husebye (1994) also described reflectors along the northwest side of the Permian Skagerrack graben of Scandinavia with apparent dips in the direction of extension. Lie and Husebye (1994) interpreted these to be a reactivated preextension fabric. An arch is imaged beneath the southern segment of the Skagerrack graben (Lie and Husebye, 1994), and it is under dipping reflectors, simi-

lar to the relation shown in Figure 10. We suggest that the ACCRETE-imaged west-dipping reflectors are normal sense shear zones that helped transfer strain from the brittle region of the crust, where the grabens occur, down into the region of ductile flow (below ~5 s TWTT).

Reflection seismic profiles over extended continental crust typically show a reflective zone in the lower crust, as seen in Figures 8 and 9, extending to the Moho (e.g., Allmendinger et al., 1987; Peddy and Hobbs, 1987; Holbrook, 1990; Holbrook et al., 1991). In the northern Basin and Range province these features have been attributed to combinations of ductile flow in felsic crust and basalt sills intruded during extension (Holbrook et al., 1991). Adams et al. (1997) attributed subhorizontal crustal reflectivity to layering in mafic intrusions, based on correlation of seismic data with lithologies found in a drill core. In the study by Adams et al. (1997), the average seismic velocities are similar to those found by Morozov et al. (2003)

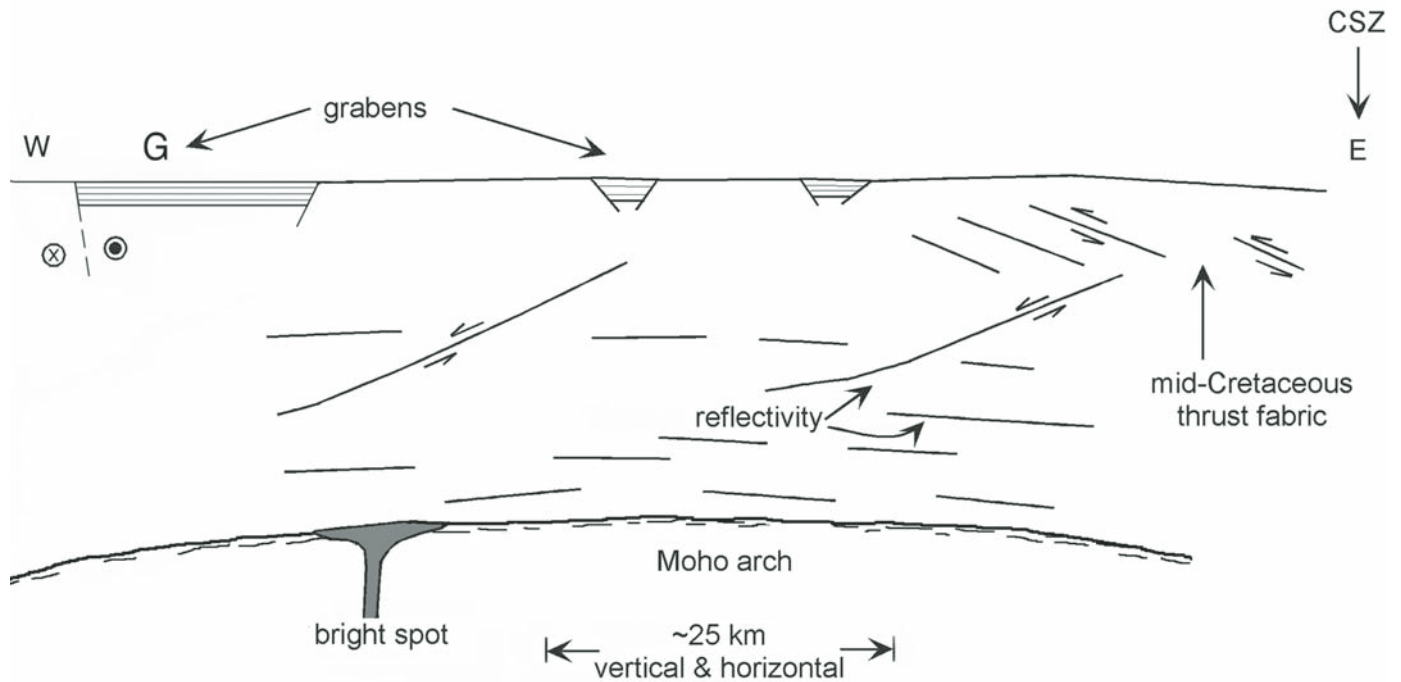


Figure 10. Interpretative sketch of east-west seismic profiles, based mainly on data from line 1255 (Fig. 6), showing the reflective Moho, arch of Moho, bright reverberant interval (bright spot) on Moho, grabens, packages of west-dipping reflecting horizons interpreted as normal sense shear zones, and middle to lower crustal subhorizontal reflectivity. Northwest-trending dextral component of offset is shown on the western side of the western graben. These features are consistent with an interpretation of extension of the whole crust in an east-west direction. In addition, east-dipping reflectors at the eastern end of section are interpreted to be due to west-verging, mid-Cretaceous thrusts. CSZ—Coast shear zone. The graben labeled “G” refers to the graben G in Figs. 2 and 3.

in the lower crust of the Insular superterrane, that correspond to gabbro. Thus, some of the lower crustal reflectivity in our study area could be due to layering in gabbro intrusions accentuated by shear strain. However, lower crustal reflectivity is most prominent in the eastern portion of our study area, where the seismic data of Morozov et al. (2001) indicate most of the crust is felsic (Fig. 4, for the mid-Cretaceous thrust belt at and southeast of the Coast shear zone), and therefore more likely to show features attributable to ductile flow of felsic rock.

The wide-angle reflection-refraction experiment (Morozov et al., 1998, 2001) imaged a pronounced arch in the Moho immediately west of the Coast shear zone (Figs. 3 and 4). The apex of this Moho arch is at a depth of 23 km. The depth to Moho increases to 26 km toward the southwest limit of the wide-angle model (CDP 2700 on line 1253; Fig. 8). The dip of the west side of this arch is continuous with the east-dipping wide-angle reflecting horizons (<3 s TWTT; Fig. 4) that Morozov et al. (2001) interpreted to be a mid-Cretaceous thrust fabric. This fabric, which is also seen at the eastern end of line 1255 (Fig. 6), may have

controlled the location of shear at this location during the late Tertiary extension.

The location and orientation of the large northwest-trending graben (G in Figs. 2, 3, and 10) suggest that its orientation may have been controlled by a preexisting weakness in the crust created by one or more of the Mesozoic sinistral shear zones and/or the Wrangellia-Alexander terrane boundary that project into it (Fig. 1; Chardon et al., 1999). The shear zones and the graben are subparallel to the Coast shear zone and the late Miocene dextral shears within the Coast shear zone (location B; Fig. 2). The age and kinematics of the late Miocene dextral shears are compatible with late Tertiary east-west extension. Chardon et al. (1999, p. 284) described late dextral shearing where the northeast side of the graben comes onshore south of the study area, and suggested that this displacement represents partitioning of slip during the Miocene transtension. Morozov et al. (2001) interpreted an apparent offset across the west side of the graben, within the study area, of an off-line wide-angle reflector to be due to dextral shear during transtension. Dextral offset across the graben is schematically noted in Figure 10.

Lowe and Dehler (1995) used gravity to model crustal thickness from Hecate Strait south through Queen Charlotte Sound. The model is constrained by seismic refraction data from that region (Spence and Asudeh, 1993). They described an arch in the Moho in northern Hecate Strait with depth to the Moho of 26 km; it is located (Fig. 3) at $\sim 131.7^{\circ}$ – 131.5° W and 54° N, and deepens eastward to 30 km at the limit of their model at 131° W and 54° N (Fig. 3).

East of the Coast shear zone, the thickness under the Coast Mountains batholith, prior to the late Tertiary extension was 34 km. This is based on an average of 2 km height of the mountains added to the deepest present-day Moho under the Coast Mountains batholith of 32 km below sea level (Morozov et al., 2001). The Coast Mountains east of the Coast shear zone were affected by a profound episode of early Tertiary extension while the rocks there were partially melted (Andronicos et al., 2003). Accordingly, it is reasonable to assume that Moho was relatively flat and 34 km deep following this event. Assuming no discontinuity across the Coast shear zone prior to the late Tertiary extension, a preextension depth to Moho across the Coast

Mountains and Insular superterrane was 34 km. This is the same thickness used by Dehler et al. (1997), based on similar reasoning, for calculating extension in Hecate Strait and Queen Charlotte Sound. However, we have no data that show that the crust west of the Coast shear zone was at the same thickness as that east of the Coast shear zone following the early Tertiary extension event.

The crust might have thinned the most during extension where there were preexisting zones of weakness. For example, the prominent arch near the Coast shear zone (Figs. 3 and 4) is clearly spatially related to the Coast shear zone as well as to the mid-Cretaceous thrusts. In addition, the arches on profile 1261 and off the northeast tip of Graham Island are near to where the Alexander-Wrangellia terrane boundary and the Mesozoic sinistral shear zones project (Fig. 1).

The pattern of relief on the Moho (Fig. 3) in the study area is suggestive of a pinch and swell structure. The stronger mantle lithosphere appears to bulge up under the arches and the weaker crust to pinch down between the arches. Such a pattern can be visualized as forming at the top of the lithospheric mantle during extension; the lithospheric mantle would be stronger than the crust above and the asthenosphere below. However, it is possible that some apparent topography on the Moho may be due to unrecognized local variations in velocity structure.

CONCLUSIONS

We identified several elements attributable to east-west extension during the late Tertiary in east Dixon Entrance, near Prince Rupert, British Columbia. The elements are seismically reflective lower crust and Moho; a pinch and swell structure defined by the Moho, which ranges from 23 to 30 km deep in the study area (Fig. 3); west-dipping reflecting horizons from ~9–15 km depth through the middle crust that we attribute to the transfer of strain from the brittle upper crust into the ductile lower crust; grabens as much as 3 km deep in the upper crust; and intervals of high-amplitude reflectivity at and below the Moho, which may be the result of basaltic magmatism that was focused into zones of weakness during extension.

The late Tertiary extension of our study area is inferred to have affected a preextension crust with a thickness of ~34 km. Where this crust was reduced in thickness to 25 km, the amount of apparent thinning was a minimum of 30%. A greater amount of thinning could have occurred if the crust had been inflated by additions of basalt dikes and sills during extension. The period of east-west extension appears to have been between 40 and 20 Ma.

Based on an integration of our MCS results with the geological and geophysical interpretations of the ACCRETE project, we suggest that there is a correlation of the pattern of late Tertiary crustal thinning to features inherited from the earlier geologic history, namely preexisting zones of weakness such as the Coast shear zone and the Mesozoic transcurrent and thrust shear zones west of the Coast shear zone.

ACKNOWLEDGMENTS

Many people and organizations helped with the navigation of the R/V *Maurice Ewing* and the logistic and permitting tasks associated with firing airguns in the inland waterways of Alaska and British Columbia. Captain Ian Young and his crew provided exceptional service. The science team on board included George Gehrels, Bill Clement, Anne Trehu, Kristin Rohr, and Carmel Lowe. Environmental observers were Sally Mizroch and George Gosnell. Glenn Woodsworth directed the small boat to intercept fishing boats from crossing the 3-km-long line of hydrophones. The Canadian Coast Guard provided immeasurable assistance. Peter Carrol of Lithoprobe directed the formal permitting process. The manuscript was much improved as a result of discussions and review by Chris Andronicos, and journal reviewers Scott Smithson, Fred Cook, Phil Hammer, Randy Keller, and anonymous. The authors' support was from the National Science Foundation Continental Dynamics program, grants EAR-92-19294 and EAR-95-26531 (Hollister) and EAR-92-19002 and EAR-95-27293 (Diebold).

REFERENCES CITED

- Adams, D.C., Miller, K.C., and Kargi, H., 1997, Reconciling physical properties with surface seismic data from a layered mafic intrusion: *Tectonophysics*, v. 271, p. 59–74, doi: 10.1016/S0040-1951(96)00219-3.
- Allmendinger, R.W., Hauge, T.A., Hauser, E.C., Potter, C.J., Klemperer, S.L., Nelson, K.D., Knuepfer, and Oliver, J., 1987, Overview of the COCORP 40°N Transect, western United States: The fabric of an orogenic belt: *Geological Society of America Bulletin*, v. 98, p. 308–319.
- Andronicos, C.L., Chardon, D.H., Hollister, L.S., Gehrels, G.E., and Woodsworth, G.J., 2003, Strain partitioning in an obliquely convergent orogen, plutonism, and synorogenic collapse: Coast Mountains batholith, British Columbia, Canada: *Tectonics*, v. 22, p. 1012–1035, doi: 10.1029/2001TC001312.
- Brady, R., Wernicke, B., McNutt, M., Mutter, J., and Correa, G., 2000, Results of the Basin and Range Geoscientific Experiment (BARGE): A marine-style seismic reflection survey across the eastern boundary of the central Basin and Range Province: *Geochemistry, Geophysics, Geosystems*, v. 1, no. 9, doi: 10.1029/2000GC000078.
- Chardon, D., Andronicos, C.L., and Hollister, L.S., 1999, Large-scale transpressive shear zone patterns and displacements within magmatic arcs: The Coast Plutonic Complex, British Columbia: *Tectonics*, v. 18, p. 278–292, doi: 10.1029/1998TC900035.
- Crawford, M.L., Hollister, L.S., and Woodsworth, G.J., 1987, Crustal deformation and regional metamorphism across a terrain boundary, Coast Plutonic Complex, British Columbia: *Tectonics*, v. 6, p. 343–361.
- Das, T., 1997, Crustal structure of western North America using surface waves and marine multichannel seismic reflection data [Ph.D. thesis]: Princeton, New Jersey, Princeton University, 115 p.
- Davidson, C., Davis, K.J., Bailey, C.M., Tape, C.H., Singleton, J., and Singer, B., 2003, Age, origin, and significance of brittle faulting and pseudotachylite along the Coast shear zone, Prince Rupert, British Columbia: *Geology*, v. 31, p. 43–46, doi: 10.1130/0091-7613(2003)031<0043:AOASOB>2.0.CO;2.
- Dehler, S.A., Keen, C.E., and Rohr, K.M.M., 1997, Tectonic and thermal evolution of Queen Charlotte Basin: Lithospheric deformation and subsidence models: *Basin Research*, v. 9, p. 243–261, doi: 10.1046/j.1365-2117.1997.00043.x.
- Evenchick, C.A., Crawford, M.L., McNicoll, V.J., Currie, L.D., and O'Sullivan, P.B., 1999, Early Miocene or younger normal faults and other Tertiary structures in west Nass River map area, northwest British Columbia, and adjacent parts of Alaska, in *Current research: Geological Survey of Canada Paper 99-1A*, p. 1–11.
- Gareau, S.A., Woodsworth, G.J., and Rickli, M., 1997, Regional geology of the northeastern quadrant of Terrace map area, west-central British Columbia, in *Current research: Geological Survey of Canada Paper 1997-A*, p. 47–55.
- Gehrels, G.E., 2001, Geology of the Chatham Sound region, southeast Alaska and coastal British Columbia: *Canadian Journal of Earth Sciences*, v. 38, p. 1579–1599, doi: 10.1139/cjes-38-11-1579.
- Hammer, P.T.C., and Clowes, R.M., 1997, Moho reflectivity patterns—A comparison of Canadian LITHOPROBE transects: *Tectonophysics*, v. 269, p. 179–198, doi: 10.1016/S0040-1951(96)00164-3.
- Hammer, P.T.C., and Clowes, R.M., 2004, Accreted terranes of northwestern British Columbia, Canada: Lithospheric velocity structure and tectonics: *Journal of Geophysical Research*, v. 109, doi: 10.1029/2003JB002749.
- Hammer, P.T.C., Clowes, R.M., and Ellis, R.M., 2000, Crustal structure of NW British Columbia and SE Alaska from seismic wide-angle studies: Coast Plutonic Complex to Stikinia: *Journal of Geophysical Research*, v. 105, p. 7961–7981, doi: 10.1029/1999JB900378.
- Hickson, C.J., 1991, The Masset Formation on Graham Island, Queen Charlotte Islands, British Columbia, in Woodsworth, G.J., ed., *Evolution and hydrocarbon potential of the Queen Charlotte Basin, British Columbia: Geological Survey of Canada Paper 90-10*, p. 305–324.
- Holbrook, W.S., 1990, The crustal structure of the Northwestern Basin and Range Province, Nevada, from wide-angle seismic data: *Journal of Geophysical Research*, v. 95, p. 21,843–21,869.
- Holbrook, W.S., Catchings, R.D., and Jarchow, C.M., 1991, Origin of deep crustal reflections: Implications of coincident seismic refraction and reflection data in Nevada: *Geology*, v. 19, p. 175–179, doi: 10.1130/0091-7613(1991)019<0175:OODCRI>2.3.CO;2.
- Hollister, L.S., 1982, Metamorphic evidence for rapid (2 mm/yr) uplift of a portion of the Central Gneiss Complex, Coast Mountains: B.C. *Canadian Mineralogist*, v. 20, p. 319–332.
- Hollister, L.S., and Andronicos, C.L., 2006, The formation of new continental crust in western British Columbia during transpression and transtension: *Earth and Planetary Science Letters*, v. 249, p. 29–38, doi: 10.1016/j.epsl.2006.06.042.
- Hurich, C.A., 1991, Source-generated noise in marine seismic profiles: The limits of reflection detectability in the upper crust, in Meissner, R., et al., eds., *Continental lithosphere: Deep seismic reflections: American Geophysical Union Geodynamics Series*, v. 22, p. 443–450.
- Hurich, C.A., 1996, Kinematic evolution of the lower plate during intracontinental subduction: An example from the Scandinavian Caledonides: *Tectonics*, v. 15, p. 1248–1263, doi: 10.1029/96TC00828.
- Hurich, C.A., and Roberts, D., 1997, A seismic reflection profile from Stjordalen to Outer Fosen, central Norway; a note on the principal results: *NGU Bulletin*, v. 433, p. 18–19, ISSN: 0332-5768.
- Hutchison, W.W., 1982, Geology of the Prince Rupert-Skeena map area, British Columbia: *Geological Survey of Canada Memoir 394*, 116 p.
- Hyndman, R.D., and Hamilton, T.S., 1993, Queen Charlotte area Cenozoic tectonics and volcanism and their association with relative plate motions along the northeastern Pacific margin: *Journal of Geophysical Research*, v. 98, p. 14,257–14,277.
- Klepeis, K.A., Crawford, M.L., and Gehrels, G.E., 1998, Structural history of the crustal-scale Coast Shear Zone north of Portland Canal, southeast Alaska and

- British Columbia: *Journal of Structural Geology*, v. 20, p. 883–904, doi: 10.1016/S0191-8141(98)00020-0.
- Lassiter, J.C., DePaolo, D.J., and Mahoney, J.J., 1995, Geochemistry of the Wrangellia flood basalt province: Implications for the role of continental and oceanic lithosphere in flood basalt genesis: *Journal of Petrology*, v. 36, p. 983–1009.
- Lie, J.E., and Husebye, E.S., 1994, Simple-shear deformation of the Skagerrak lithosphere during the formation of the Oslo Rift: *Tectonophysics*, v. 232, p. 133–141, doi: 10.1016/0040-1951(94)90080-9.
- Lowe, C., and Dehler, S.A., 1995, Crustal structure beneath Queen Charlotte basin, Canada: Results of seismically constrained gravity inversion: *Journal of Geophysical Research*, v. 100, p. 24,331–24,345, doi: 10.1029/95JB01874.
- Morozov, I.B., Smithson, S.B., Hollister, L.S., and Diebold, J.B., 1998, Wide-angle seismic imaging across accreted terranes, southeastern Alaska and western British Columbia: *Tectonophysics*, v. 299, p. 281–296, doi: 10.1016/S0040-1951(98)00208-X.
- Morozov, I.B., Smithson, S.B., Chen, J., and Hollister, L.S., 2001, Generation of new continental crust and terrane accretion in southeastern Alaska and western British Columbia: Constraints from P- and S-wave wide-angle data (ACCRETE): *Tectonophysics*, v. 341, p. 49–67, doi: 10.1016/S0040-1951(01)00190-1.
- Morozov, I.B., Christensen, N.L., Smithson, S.B., and Hollister, L.S., 2003, Seismic and laboratory constraints on crustal formation in a former continental arc (ACCRETE, southeastern Alaska and western British Columbia): *Journal of Geophysical Research*, v. 108, no. B1, 9 p., doi:10.1029/2001JB001740.
- Peddy, C.P., and Hobbes, R.W., 1987, Lower crustal reflectivity of the continental margin southwest of Britain: *Annales Geophysicae*, v. 5B, p. 331–338.
- Rohr, K.M.N., and Currie, L., 1997, Queen Charlotte Basin and Coast Mountains; paired belts of subsidence and uplift caused by a low-angle normal fault: *Geology*, v. 25, p. 819–822, doi: 10.1130/0091-7613(1997)025<0819:QCBACM>2.3.CO;2.
- Rohr, K.M.M., and Dietrich, J.R., 1992, Strike-slip tectonics and development of the tertiary Queen Charlotte Basin, offshore western Canada: Evidence from seismic reflection data: *Basin Research*, v. 4, p. 1–19, doi: 10.1111/j.1365-2117.1992.tb00039.x.
- Rohr, K.M.M., Scheidhauer, M., and Trehu, A.M., 2000, Transpression between two warm mafic plates: The Queen Charlotte Fault revisited: *Journal of Geophysical Research*, v. 105, p. 8147–8172, doi: 10.1029/1999JB900403.
- Rubin, C.M., and Saleeby, J.B., 1992, Tectonic history of the eastern edge of the Alexander terrane, southeast Alaska: *Tectonics*, v. 11, p. 586–602.
- Shillington, D.J., Van Avendonk, H.J.A., Holbrook, W.S., Kelemen, P.B., and Hornbach, M.J., 2004, Composition and structure of the central Aleutian island arc from arc-parallel wide-angle seismic data: *Geochemistry, Geophysics, Geosystems*, v. 5, Q10006, doi: 10.1029/2004GC000715.
- Spence, G.D., and Asudeh, I., 1993, Seismic velocity structure of the Queen Charlotte Basin beneath Hecate Strait: *Canadian Journal of Earth Sciences*, v. 30, p. 787–805.
- Spence, G.D., and Long, D.T., 1995, Transition from oceanic to continental crustal structure: Seismic and gravity constraints at the Queen Charlotte transform margin: *Canadian Journal of Earth Sciences*, v. 32, p. 699–717.
- Stock, J.M., and Molnar, P., 1988, Uncertainties and implications of the Late Cretaceous and Tertiary position of North America relative to the Farallon, Kula, and Pacific plates: *Tectonics*, v. 7, p. 1339–1384.
- van der Heyden, P., Woodsworth, G.J., and Snyder, L.D., 2000, Reconnaissance geological mapping in southwest Nass River map area, British Columbia, in *Current research: Geological Survey of Canada Paper 2000-A6*, 8 p.
- Wheeler, J.O., and McFeely, P., compilers, 1991, Tectonic assemblage map of the Canadian Cordillera and adjacent parts of the United States of America: Geological Survey of Canada Map 1712A, scale 1:2,000,000.
- Woodsworth, G.J., 1991, Neogene to recent volcanism along the east side of Hecate Strait, British Columbia, in Woodsworth, G.J., ed., *Evolution and hydrocarbon potential of the Queen Charlotte Basin*, British Columbia: Geological Survey of Canada Paper 90-10, p. 325–335.

MANUSCRIPT RECEIVED 31 JULY 2007

REVISED MANUSCRIPT RECEIVED 22 OCTOBER 2007

MANUSCRIPT ACCEPTED 18 NOVEMBER 2007